NASA TECHNICAL NOTE

NASA TN D-2704

NASA TN D-2704

HEMISPHERICAL SPECTRAL EMITTANCE OF ABLATION CHARS, CARBON, AND ZIRCONIA TO 3700° K

by R. Gale Wilson

Langley Research Center
Langley Station, Hampton, Va.

NATIONAL AERONAUTICS AND SPACE ADMINISTRATION • WASHINGTON, D. C. • MARCH 1965

HEMISPHERICAL SPECTRAL EMITTANCE OF ABLATION CHARS, CARBON, AND ZIRCONIA TO 3700° K

By R. Gale Wilson

Langley Research Center
Langley Station, Hampton, Va.

NATIONAL AERONAUTICS AND SPACE ADMINISTRATION

For sale by the Office of Technical Services, Department of Commerce,
Washington, D.C. 20230 -- Price $2.00

HEMISPHERICAL SPECTRAL EMITTANCE OF ABLATION CHARS, CARBON, AND ZIRCONIA TO 3700° K*

By R. Gale Wilson
Langley Research Center

SUMMARY

The initial results of the application of special optical techniques to high-temperature emittance and reflectance studies of an ablation-material char and certain other refractory materials representative of those present in ablation residues formed during aerospace reentry operations are presented. Spectral hemispherical emittance and reflectance were determined with an image pyrometer integrated with an arc-imaging furnace for carbon, graphite, zirconia, and a phenolic-nylon ablation-material char at wavelengths from 0.37 μm to 0.72 μm for temperatures from 2100° K to 3700° K. The data obtained are compared with those of other investigations to the extent that the existence of comparable data permits.

Surface-roughness properties of the materials studied were determined from measurements made with a light-section microscope. The dependence of the spectral hemispherical emittance of oxidized carbon at a wavelength of 0.65 μm on its surface-roughness properties was investigated experimentally and the emittance was found to be a linear function of the root-mean-square slope of the surface when the roughness is large compared with wavelength.

INTRODUCTION

At velocities associated with reentry into the earth's atmosphere from earth-orbital or outer-space missions, flight vehicles experience aerodynamic heating which produces surface temperatures above the melting or vaporization temperatures of conventional structural materials. Thermal protection systems have been devised in which ablating materials are used effectively to protect the load-carrying structures of these vehicles. Charring ablation materials have been shown to be particularly effective for use in thermal protection systems (refs. 1 and 2) because of their ability to reradiate a significant portion of the heat absorbed. In order to evaluate the radiation-cooling effectiveness of charring ablators, their total hemispherical emittance at performance temperatures must be known. The absorptance of charring ablators in the ultraviolet

*The information presented herein was offered as a thesis in partial fulfillment of the requirements for the degree of Master of Arts in Physics, College of William and Mary, Williamsburg, Virginia, August 1964.

and visible parts of the spectrum is also important to their performance for certain types of reentry operation, that is, for reentry characterized by significant radiative heating of the vehicle by ultraviolet and visible radiation from shock-heated air. (See ref. 3.)

The object of the present investigation was to obtain hemispherical spectral emittance, absorptance, and reflectance data at high temperatures on the char of an ablation material and on certain other refractory materials representative of the class of materials present in ablation residues formed during aerospace reentry operations. In order to circumvent some of the problems of radiation measurement and temperature measurement associated with extending the use of conventional methods of measurement to high temperatures, special optical techniques were applied in this investigation. An apparatus consisting of an image pyrometer integrated with a double-ellipsoidal-mirror arc-imaging furnace was used for heating the material samples and for measuring spectral reflectance and temperature. Spectral emittance was calculated from the reflectance measurements. Several filter-detector systems were selected for a range of wavelengths covering the visible spectrum and extending into the near ultraviolet spectrum. Suitable attenuation of the arc irradiation of the sample provided for sample surface temperatures from about 2100° K to 3700° K.

Special consideration was given to surface characterization of the materials studied. Surface-roughness properties were determined from surface-profile measurements made with a light-section microscope, and pore-size spectra were determined for the porous materials by a mercury-intrusion method.

The International System of Units (SI) is used throughout this report. (See ref. 4.) In SI units, the familiar wavelength unit μ (micron) is designated by μm (micrometer).

SYMBOLS

A	oscillograph signal for arc light
c_1	first radiation constant, watts-$\mu m^4/m^2$
c_2	second radiation constant, μm-°K
E	photomultiplier output for emitted light from sample or standard lamp
h	surface-profile height
i	incident light on element of sample surface
K	combined constant of optical system
k	constant of filter-detector system, per °K
n	summation index

R	photomultiplier output for reflected light from sample
r	reflected light from element of sample surface
T	temperature
W	hemispherical spectral radiant intensity per unit area of sample or standard lamp, watts/m^2-μm
Δx	small increment of length along nominal (average) surface of material
Δy	small increment of length perpendicular to nominal surface of material
α	hemispherical absorptance
ϵ	hemispherical emittance
λ	wavelength, μm (1 μm = 1 micron)
ρ	hemispherical reflectance

Subscripts:

1	higher (temperature) or first (radiation constant)
2	lower (temperature) or second (radiation constant)
a	apparent
L	standard lamp
S	material sample
t	true
λ	spectral

A prime is used to denote values corrected for errors due to rapid cooling.

TEST APPARATUS AND SAMPLES

Apparatus for Measurement of Reflectance and Temperature

Imaging furnace and pyrometer.- The arc-imaging furnace used in this investigation is described by Glaser in reference 5 and the image pyrometer and its principles of operation are described by Comstock in reference 6. Briefly, the arc-imaging furnace, shown schematically in figure 1, consists of an optical system having two 52-centimeter-diameter ellipsoidal mirrors located coaxially and facing each other at a distance of approximately 2 meters. Their major and

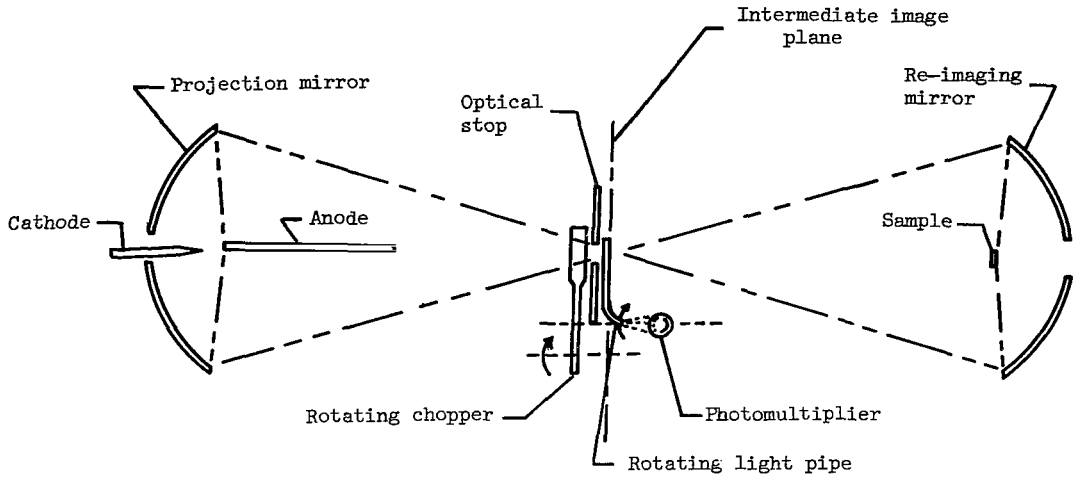

Figure 1.- Schematic of arc-imaging furnace with image pyrometer.

minor focal lengths are 104 centimeters and 20 centimeters, respectively. An electric-arc radiation source is located at the minor focal point of one mirror and its image is formed at the minor focal point of the other mirror, after two reflections of the arc radiation.

The image pyrometer, illustrated schematically in figure 2, is an instrument designed to obtain radiation measurements in the intermediate image plane where the major focuses of the mirrors coincide and where magnified images of the arc and sample are formed. The image pyrometer consists principally of two light pipes, a chopper, an optical filter, and a photomultiplier. The light pipes are L-shaped, each constructed from platinum tubing enclosing a single filament of quartz. One tube has an aperture facing the sample and the other, an aperture facing the arc. The light pipes are mounted in a common hub, and as it rotates the light pipes scan periodically through the arc and sample images and transmit light from the images to the photomultiplier via the filter. The output of the photomultiplier is amplified and read out on an oscillograph recorder in the form of radiation profiles across the diameters of arc and sample images. The rapidly rotating chopper is synchronized with the light pipes to permit the sample-oriented light pipe to view the sample image alternately with the arc radiation incident on the sample and with the arc radiation briefly obstructed from the sample. A reduced tracing of a typical oscillogram for carbon (T_S = 3100° K; λ = 0.72 μm), together with an enlarged view of the central part of the radiation profile, is shown in figure 3. From the radiation measurements on the sample with the chopper alternately open and closed, $E_{\lambda,S} + R_{\lambda,S}$ and $E_{\lambda,S}$, respectively, along with measurements on a standard-temperature source and a reflectance standard separately substituted for the sample, the temperature and reflectance of the sample at every point across its irradiated surface can be determined.

Optical filters.- A set of five filters was used to make reflectance measurements over a range of wavelengths that included the visible spectrum and extended into the near ultraviolet spectrum. In the set there were two glass

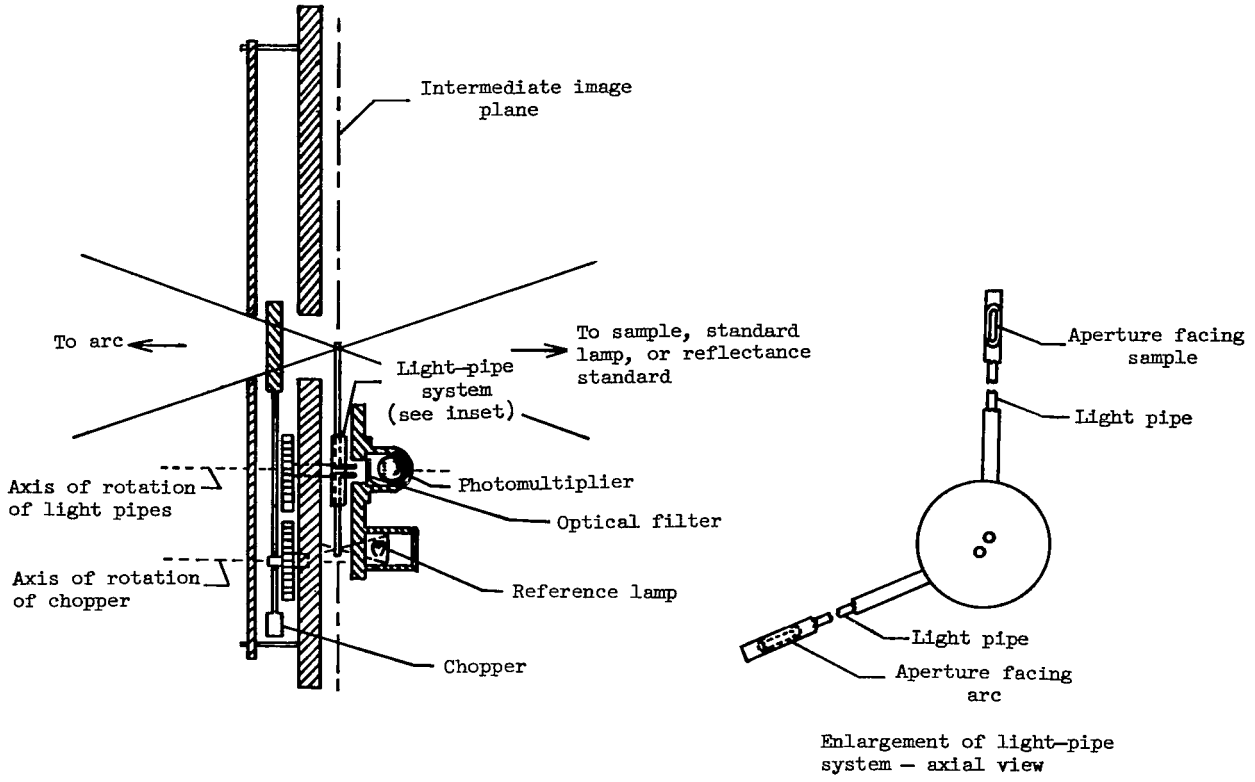

Figure 2.- Image pyrometer operating mechanism.

filters, one single-film gelatin filter, and two gelatin filters each of which was constructed by superimposing two single gelatin films. The gelatin film in each case was mounted in Canada balsam cement between two thin layers of optically flat glass. Tests were made to assure that the temperature in the filter receptacle of the pyrometer stayed within safe limits for use of the gelatin filters during furnace operation. Table 1 presents certain properties of the filters and the filter-detector systems.

Temperature modulation.- In order to cover a range of sample temperatures, neutral-density filters were constructed of standard 10- and 20-mesh brass cloth to reduce the intensity of irradiation of the sample. Each wire-cloth filter was mounted on a ring designed to fit the circumference of the mirror at the arc end of the furnace, with a 15-centimeter hole in the region of the arc. With or without a filter, the temperature distribution across the diameter of the sample approximates a Gaussian shape, with the temperature decreasing from a maximum value at the center of the sample to about 75 percent of the maximum at a radius of about 0.5 centimeter, corresponding to the periphery of the arc image. The measurements of reflectance and temperature were obtained in every case in the region of the maximum temperature of the sample, and, except for one particular series of tests whose exception will be explained later, after the sample had attained a steady state. The purpose of this particular method of attenuation of the arc irradiation was to preserve the hemispherical character of the measurements and to avoid shadowing either of the intermediate images. It was

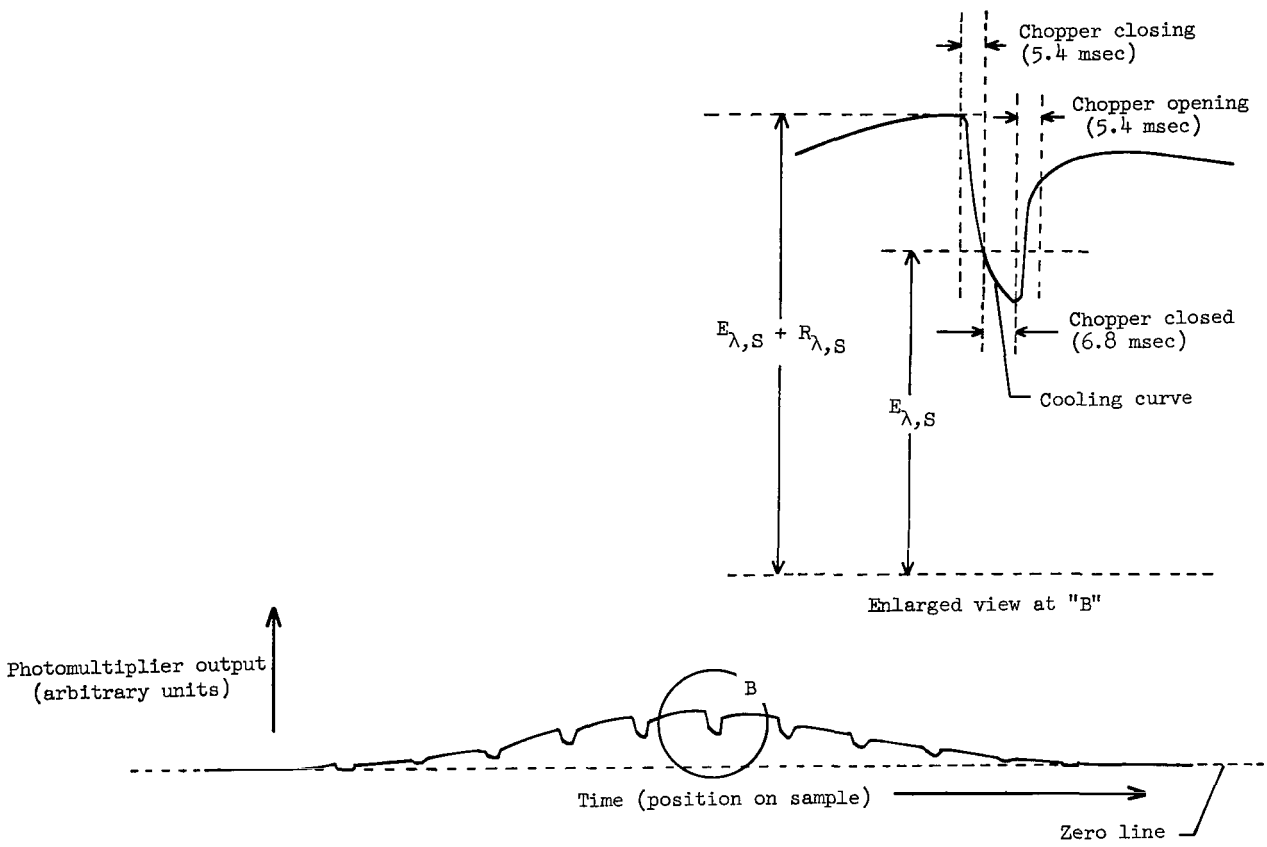

Figure 3.- Image pyrometer oscillogram for carbon.

TABLE 1.- PROPERTIES OF FILTERS AND DETECTORS

Type of filter	Spectral response curve of photomultiplier	Half-bandwidth for filter-photomultiplier system, μm	Effective wavelength, μm
Glass	S-4	0.040	0.366
Gelatin film	S-4	.029	.459
Gelatin film	S-4	.021	.560
Glass	S-4	.029	.650
Gelatin film	S-8	.070	.716

believed that this approach to temperature control would yield more reliable and consistent data than those obtainable from measurements during temperature rise of the sample or from measurements made at points other than the maximum-temperature region on the surface of the sample.

Test Samples

Samples of all the materials studied were disks 1.3 centimeters in diameter and 0.5 centimeter in thickness. For each reflectance and temperature measurement, one of the disks was mounted in a small steel block, supported in and insulated from the block by four equally spaced spring-loaded zirconia pins which were tapered at the points of contact with the periphery of the sample. Measurements were made on the circular face of the disk which was located in the minor focal plane of the reimaging mirror, with its center on the optical axis of the arc-imaging furnace mirrors.

Apparatus for Measurement of Sample Surface Properties

Inasmuch as the emittance of any material is expected to be variable with surface roughness, it was considered desirable in this investigation to define the microgeometry of the surfaces of the materials for which emittance was determined. A light-section microscope was chosen for making the measurements because it permits measurements on soft materials without destroying or altering the surface and because it is suitable for the determination of several surface parameters. One arrangement for use of the light-section method to measure surface roughness is described in reference 7. The optical arrangement of the instrument employed in the present study is shown in figure 4(a). An incandescent lamp illuminates a slit which, by means of an objective, is reproduced on the surface under study as a thin band of light. The band of light illuminates the surface along its contour, and a profile image of the surface may be observed and/or photographed through a microscope whose objective has the same magnification as that of the illuminating objective. Illumination and observation directions form a 90° angle with each other and a 45° angle with the surface being examined. A crosshair, visible in the eyepiece, may be shifted within the field of view by means of a micrometer drum. Because the light band meets the surface at an angle of 45° and is observed at a right angle to this direction, an apparent profile height h_a (fig. 4(b)) is observed instead of the true profile height h_t. Obviously, $h_a = \sqrt{2}h_t$, but the factor $\sqrt{2}$ is accounted for in the calibration of the crosshair which makes possible direct reading of the height and longitudinal location of each observed point of the profile. The range of the instrument permits measurements of surface irregularities for which h_t varies from 1 to 400 μm.

Apparatus for Measurement of Sample Porosity

The very porous nature and precipitous surfaces of some of the materials studied precluded obtaining meaningful surface-roughness measurements on them with the light-section microscope because of the formation of discontinuous

profile images. Since the surface characteristics of porous materials are closely related to their porosity, pore-size spectra were determined for the appropriate materials. A mercury-intrusion method described in reference 8 was employed to make the measurements. Briefly, the method is based on the negative capillarity of mercury; that is, mercury must be forced into a porous material and the pressure required is determined by the surface tension of the mercury, the wetting angle, and the diameter of the smallest pore filled at that pressure. The instrument is designed for forcing mercury into the pores of a sample material at pressures ranging from subatmospheric to 3.5×10^7 N/m^2 and simultaneously indicating the volume of mercury absorbed at any given pressure, thus determining the pore-size spectrum of the sample for pore sizes ranging from 0.035 to 100 μm.

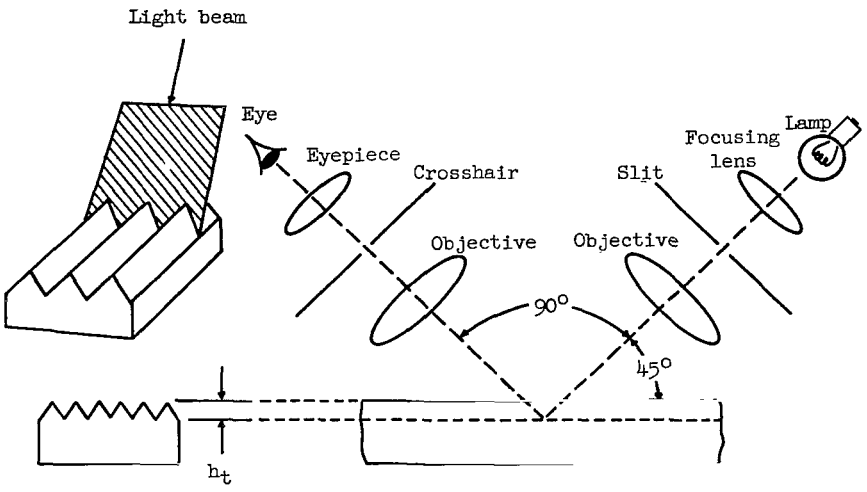

(a) Optical arrangement.

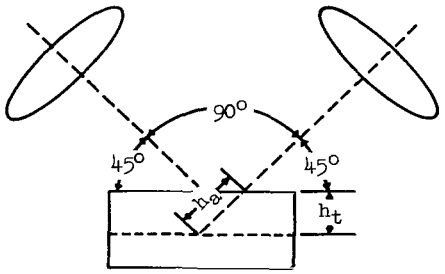

(b) Principle of measurement.

Figure 4.- Operation principles of light-section microscope.

TEST METHODS

Method of Reflectance Measurement

In the following discussion, the principles of operation and measurement employed by the image pyrometer given in reference 6 are summarized and the calculations involved are modified for application to measurements covering a range of wavelengths.

To determine the temperature of the sample, it is first necessary to determine its emittance. For an opaque sample,

$$\alpha_\lambda + \rho_\lambda = 1 \tag{1}$$

and from Kirchhoff's law (ref. 9) and equation (1)

$$\epsilon_\lambda = \alpha_\lambda = 1 - \rho_\lambda \tag{2}$$

The image pyrometer measures the spectral reflectance, from which the spectral emittance is calculated by equation (2) and is used in the determination of sample temperature. To accomplish the reflectance measurement, the apparatus measures sequentially the arc light, the emitted plus reflected light from the sample, and the emitted light from the sample. The difference between the last two measurements is the reflected light from the sample, if no cooling of the sample occurs during the brief time taken for the chopper to interrupt the arc irradiation of the sample. The emitted light is measured while the arc radiation is briefly obstructed by the chopper. Interruption by the chopper occurs every 67 milliseconds and the duration of each interruption is about 7 milliseconds as shown in figure 3.

From the foregoing considerations the spectral emittance of the sample may be expressed as

$$\epsilon_{\lambda,S} = 1 - \rho_{\lambda,S} = 1 - \frac{r_{\lambda,S}}{i_{\lambda,S}} = 1 - K\,\frac{\left(E_{\lambda,S} + R_{\lambda,S}\right) - E_{\lambda,S}}{A_\lambda} \tag{3}$$

The constant K includes a measure of the fraction of the light from the arc image that is incident on the sample, as well as the pyrometer sensitivity through the sample- and arc-viewing optics. This constant may be determined by replacing the sample with a water-cooled surface of known reflectance. Because the spectral reflectance of freshly deposited magnesium oxide has been extensively studied (e.g., refs. 10 to 12), it was used as a standard for determining the value of K. Its diffuse reflectance throughout the visible spectrum is about 0.97.

The reflectance measurement by the image pyrometer, including specular and diffuse components, is essentially hemispherical, since the re-imaging mirror irradiates the sample and collects reflected and emitted radiation from the sample over a solid angle of about 5.7 (1.8π) steradians. The emittance determined is essentially hemispherical, since reflectance measured under conditions of hemispherical illumination and hemispherical viewing is the complement of hemispherical emittance.

Method of Temperature Calculation

Calculation of the sample temperature requires measurement of radiation from a standard-temperature source as well as from the sample itself. A tungsten-strip lamp serves as an accurate standard radiation source. Planck's law or Wien's law may be written for the sample and for the standard lamp. Wien's law is simpler to use and was used here since it agrees within one-half

of 1 percent with Planck's law for the range of wavelengths and temperatures involved. (See ref. 13.) Wien's law for the sample is

$$W_{\lambda,S} = \epsilon_{\lambda,S} c_1 \lambda^{-5} \exp\left(-\frac{c_2}{\lambda T_S}\right) \tag{4}$$

where $W_{\lambda,S}$ is the time rate of emission of radiant energy per unit interval of wavelength throughout 2π steradians per unit area of the sample at absolute temperature T_S. Wien's law for the standard lamp is

$$W_{\lambda,L} = \epsilon_{\lambda,L} c_1 \lambda^{-5} \exp\left(-\frac{c_2}{\lambda T_L}\right) \tag{5}$$

Since the viewing optics for measuring emitted radiation is the same for both the sample and the standard lamp, the ratio of the two expressions of Wein's law is equal to the ratio of the oscillograph signals for emitted radiation from sample and lamp $E_{\lambda,S}$ and $E_{\lambda,L}$, respectively. By taking this ratio, the following expression is obtained:

$$\frac{1}{T_L} - \frac{1}{T_S} = \frac{\lambda}{c_2} \ln \frac{\epsilon_{\lambda,L} E_{\lambda,S}}{\epsilon_{\lambda,S} E_{\lambda,L}} \tag{6}$$

Solving equation (6) for T_S gives

$$T_S = \frac{T_L}{1 - k_\lambda T_L \log \frac{\epsilon_{\lambda,L} E_{\lambda,S}}{\epsilon_{\lambda,S} E_{\lambda,L}}} \tag{7}$$

where

$$k_\lambda = \frac{2.302\lambda}{c_2} = \text{Constant incorporating a change from natural to common logarithms and absorbing } \lambda/c_2 \tag{8}$$

The value of λ is a function of the filter and detector system in the pyrometer and is essentially the effective wavelength of response of the image pyrometer. The value of k_λ may be determined by operation of the pyrometer with the standard lamp set successively at two different temperatures, $T_{L,1}$ and $T_{L,2}$. The resultant expression for k_λ is

$$k_\lambda = \frac{T_{L,1} - T_{L,2}}{T_{L,1} T_{L,2} \log \frac{\epsilon_{\lambda,L,2} E_{\lambda,L,1}}{\epsilon_{\lambda,L,1} E_{\lambda,L,2}}} \tag{9}$$

The sample temperature can be determined by substitution of k_λ into equation (7) along with the oscillograph data from the lamp at either temperature.

The physical meaning of effective wavelength of response of the image pyrometer is explained in figure 5. Here the triple product of the ultraviolet-filter transmission curve, the S-4 photomultiplier relative response curve, and the relative spectral radiant intensity curve for the standard lamp determines the combined response (shown in the upper right corner of the figure) of a typical source, filter, and detector system. The effective wavelength is taken as the line dividing the area under the product curve into two equal parts. Values of λ for the five filters determined by this method were in agreement within 4.5 percent with averaged values calculated by solving equation (8) for λ and making use of the values of k_λ determined by equation (9). The effective wavelengths are only very weak functions of the source temperature for the range of sample temperatures studied and are well defined at the standard-lamp temperature of 2900° K, which is about the midpoint of the range of sample temperatures.

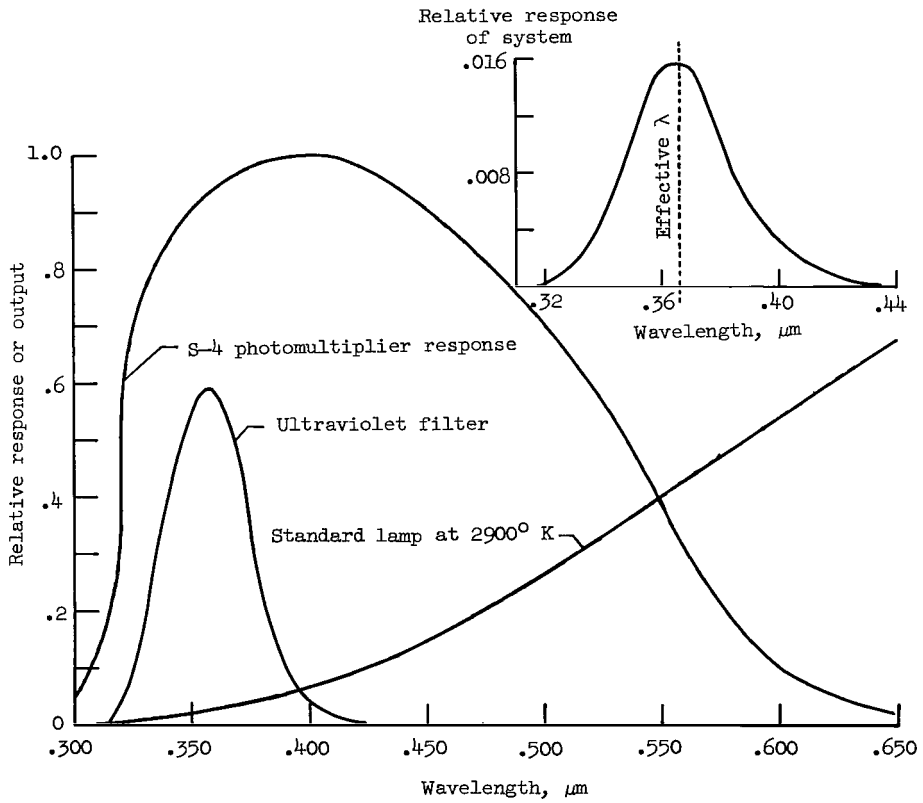

Figure 5.- Response of source-filter-detector system plotted against wavelength.

Because of the unavailability of spectral hemispherical emittance data on tungsten-strip lamps at high temperatures, spectral normal emittance data were used in equations (7) and (9). The spectral normal emissivity of tungsten ribbon filament has been the subject of considerable study because of its use as a radiation standard. The data of De Vos (ref. 14) and Larrabee (ref. 15), covering a broad range of wavelengths and temperatures, are considered the most reliable available. The data of De Vos were used herein because they include a broader temperature range. Normal and hemispherical emittances of tungsten are not equal because tungsten does not emit in accordance with Lambert's cosine law, but studies by Worthing (see ref. 16) and by Blau et al. (see ref. 17) indicate that hemispherically measured values would not be expected to be more than 6 or 7 percent greater than normally measured values.

Evaluation of Errors

Systematic errors.- Since several potential sources of error are inherent in methods of measurement of the type applied in this investigation, the most suspected ones are enumerated and evaluated either quantitatively or qualitatively. Errors in temperature measurement would be expected to be due primarily to errors in the experimentally determined emittance values, the use of normal emittance data for the standard lamp in the absence of hemispherical data, and losses due to internal reflections within the envelope of the standard lamp. However, an error of 5 percent in the emittance of the sample or standard lamp would produce an error of less than 1 percent in the temperature. The error due to applying normal emittance data to the lamp and that due to losses within the lamp tend to compensate for each other.

The possible difference between the geometrical distribution of reflected radiation from the MgO reflectance standard and that emitted and reflected by the sample might appear to introduce error into the reflectance measurements. However, error due to such a difference would be minimized, on the basis of two considerations: (1) the distribution of illumination and the collection of radiation from the reflectance standard and from the sample are both essentially hemispherical, and (2) the distributions for the reflectance standard and for the generally rough samples studied would be expected to be similar.

Error in the reflectance measurements that might be expected to result from differences in the transmission properties of the two light pipes is eliminated through the calibration constant K, assuming that any such differences remain constant for all the measurements on the sample and reflectance standard at a given wavelength.

In order to eliminate errors in the radiation measurements that might arise from drifts in the electronic equipment, the image pyrometer includes a well regulated reference lamp to permit normalizing all the measurements. The sample-oriented light pipe receives a signal from the reference lamp (fig. 2) once each cycle of rotation, and the accompanying radiation measurements are normalized to the reference lamp oscillogram.

Errors due to rapid cooling.- The most serious problem in measuring reflectance at high temperatures is separating the emitted and reflected radiation. This problem with the arc-imaging furnace arises from the inability to achieve an instantaneous interruption of the incident radiation, with consequent cooling of the sample surface during the brief time required for the edge of the chopper to traverse the aperture at the intermediate image plane. If measurements are made just at the instant that the chopper has completely eclipsed the arc, which is the earliest time in the cycle that emitted and reflected radiation are completely separated, any decrease in the emitted radiance due to cooling will be erroneously classified as reflected radiation. The magnitude of the error is in part dependent upon the thermal conductivity of the sample material, since this property determines the magnitude of the thermal gradient associated with a given amount of radiated flux from the front face of the sample.

Null and Lozier (ref. 18), recognizing that a sample in an arc-imaging furnace provides a plane surface with an essentially uniform temperature over a substantial area, have made use of solutions to the problems of one-dimensional heat conduction normal to the surface of a semi-infinite body subjected to periodic and nonperiodic step-function heat fluxes to evaluate thermal conductivity. The solutions show that, to a first-order approximation, the surface temperature after chopper interruption is directly proportional to the square root of time. Null and Lozier have also mathematically investigated the effect on the cooling curve of the finite time required to interrupt the furnace radiation by means of a mechanical chopper. This analysis showed that if time is measured from the instant when the arc is half-eclipsed, and temperature is plotted against the square root of time, the slope of the resulting straight line will be the same as that which would be obtained with a chopper fast enough to prevent any cooling during the interruption process.

The work of reference 18 provides a basis for investigating the possibility of significant errors inherent in these reflectance measurements due to a combination of high temperatures, high total emittances, rough sample surfaces with high thermal inertia, and finite chopper speed. The approach taken was first to examine the cooling curve for each sample very closely and to calculate the emittance and temperature from oscillograph measurements made at the time corresponding to completed interruption by the chopper. The time on the oscillogram corresponding to completed chopper interruption could be determined quite accurately by magnifying the cooling curve, studying it in relation to the time scale of the oscillogram, and knowing the time required for the chopper to completely interrupt the radiation and the duration of the interruption. A typical enlarged cooling curve is shown in figure 3. The photomultiplier output during the time that the chopper is closed is proportional to the spectral radiant intensity per unit area of the sample, which in turn varies linearly with the sample temperature for a small temperature change. Therefore, in accordance with the analysis of reference 18, the photomultiplier output during the time the chopper is closed would be expected to exhibit a square-root-of-time dependence if the temperature drop is sufficiently small. It was found that this was the case, when three or four points on each cooling curve were plotted against the square root of time, with time measured from the half-time point of chopper interruption. By extrapolating the straight line obtained from plotting emitted

signal against the square root of time for each sample to the half-time of chopper interruption, a new value for the emitted signal corresponding to the beginning of chopper interruption was determined, and thus a corrected emittance and temperature. To incorporate the corrections into the earlier equations, equations (3) and (7) may be rewritten

$$\epsilon'_{\lambda,S} = \frac{\left(E'_{\lambda,S} + R'_{\lambda,S}\right) - E'_{\lambda,S}}{A_\lambda} \tag{10}$$

and

$$T'_S = \frac{T_L}{1 - k_\lambda T_L \log \frac{\epsilon_{\lambda,L} E'_{\lambda,S}}{\epsilon'_{\lambda,S} E_{\lambda,L}}} \tag{11}$$

where the primed quantities denote extrapolated values. Errors due to rapid cooling were found to be significant in some cases and corrections were made for them.

From the reproducibility of the data and the earlier considerations on systematic errors, it is believed that the emittance values reported herein are generally accurate to 1 or 2 percent; however, for the highest char temperature and the two longest wavelengths, the emittance values may be as much as 3 percent low due to slight undercorrection for rapid-cooling errors. The undercorrection results because the assumption that the sample spectral radiant intensity per unit area varies linearly with temperature is only a fair approximation for the temperature range over which cooling occurs at the highest temperatures.

Method of Determining Surface Properties

One of the most formidable problem areas in the field of thermal radiation of solids is the development of theory relating the radiative and reflective properties of materials to their surface-roughness properties. Progress toward understanding this problem has been limited to special cases, with suitable assumptions about the statistical character of surfaces, because of the extreme complexity of the generalized problem and the lack of knowledge of the statistics of actual rough surfaces. A good summary of some of the early studies of the problem, including a list of references, is presented in reference 19 (pp. 293-295). Recent work by Bennett and Porteus (refs. 20 and 21), based on a statistical treatment of the reflection of electromagnetic radiation from a rough surface derived by Davies (ref. 22), has revealed certain quantitative relationships between surface character and reflectance properties. In reference 20 a theory is presented which relates the root-mean-square roughness of a plane surface with its specular reflectance at normal incidence, for the case when the roughness is small compared with the wavelength of the radiation. In

reference 21 the theory is extended with certain restrictions to shorter wavelengths. The root-mean-square roughness (ref. 23) is the root-mean-square deviation of the surface from the mean surface level. References 21 and 22 seem to be oriented toward the development of a theory to explain surface properties from the reflectance of radiation incident normally and reflected specularly. It is indicated in these references that, for angles of incidence and reflection other than normal and for surfaces with irregularities large compared with the wavelength, the root-mean-square slope is an important factor in determining the reflected radiation.

The primary concern with surface properties in this study was to characterize the surfaces of the materials studied with surface-property data pertinent to the time of reflectance measurement and meaningful with respect to the emissive and reflective properties of the materials. Since arc irradiation of the sample in every case was terminated immediately after the reflectance measurement and the sample quickly cooled to room temperature, the subsequent surface-property measurements were assumed to be reasonably representative of the surface conditions at the time of reflectance measurement. A rather arbitrary method was applied to obtain data which could be expected to be statistically valid. For carbon and zirconia the profile data were obtained for a circular area at the center of the sample surface with a diameter of about 1.3 millimeters, and profiles were examined across four diameters of the circular area displaced from one another by 45°. Constant increments Δx parallel to the nominal-surface plane and corresponding variable increments Δy perpendicular to that plane were measured to determine the slope $\Delta y/\Delta x$ of each corresponding successive section of profile. Values of Δx were small enough (12 μm) to follow the profile quite closely. For graphite, Δx increments of 6 μm were chosen and a circular area of about 0.7-millimeter diameter was studied. In every case the slopes of 400 increments were evaluated for each sample, and the root-mean-square (rms) slope was calculated by the following equation:

$$\text{rms slope} = \left[\frac{1}{400} \sum_{n=1}^{400} \left(\frac{\Delta y}{\Delta x} \right)_n^2 \right]^{1/2} \tag{12}$$

RESULTS AND DISCUSSION

Measurements on Carbon and Graphite

Wavelength and temperature dependence.- Spectral emittance and reflectance data were obtained on high-purity (less than 6 ppm impurity) spectroscopic grades of carbon and graphite at three temperature levels. To assure that all samples of each material had like surfaces before testing, the surface of each sample disk to be exposed to the furnace radiation was polished successively with 0, 3/0, and 4/0 grades of Buehler emery polishing paper. This polishing resulted in a glossy finish. Upon exposure in air to the arc-image thermal flux, this surface was quickly roughened as a result of oxidation. Each sample

was exposed long enough to attain its maximum, steady-state temperature, but not long enough to permit appreciable recession of the surface on which the image pyrometer measurements were being made. Varying arc irradiation level from conditions of no attenuation to that produced by the 20-mesh filter resulted in averaged temperatures of 3230° K, 2530° K, and 2120° K for carbon and 2990° K, 2390° K, and 2120° K for graphite. Figures 6 and 7 present the determined emittances and reflectances plotted against wavelength for each temperature and against temperature for each wavelength. Duplicate measurements were made for each set of conditions, with the exception that triplicate measurements were made on graphite at its highest temperature.

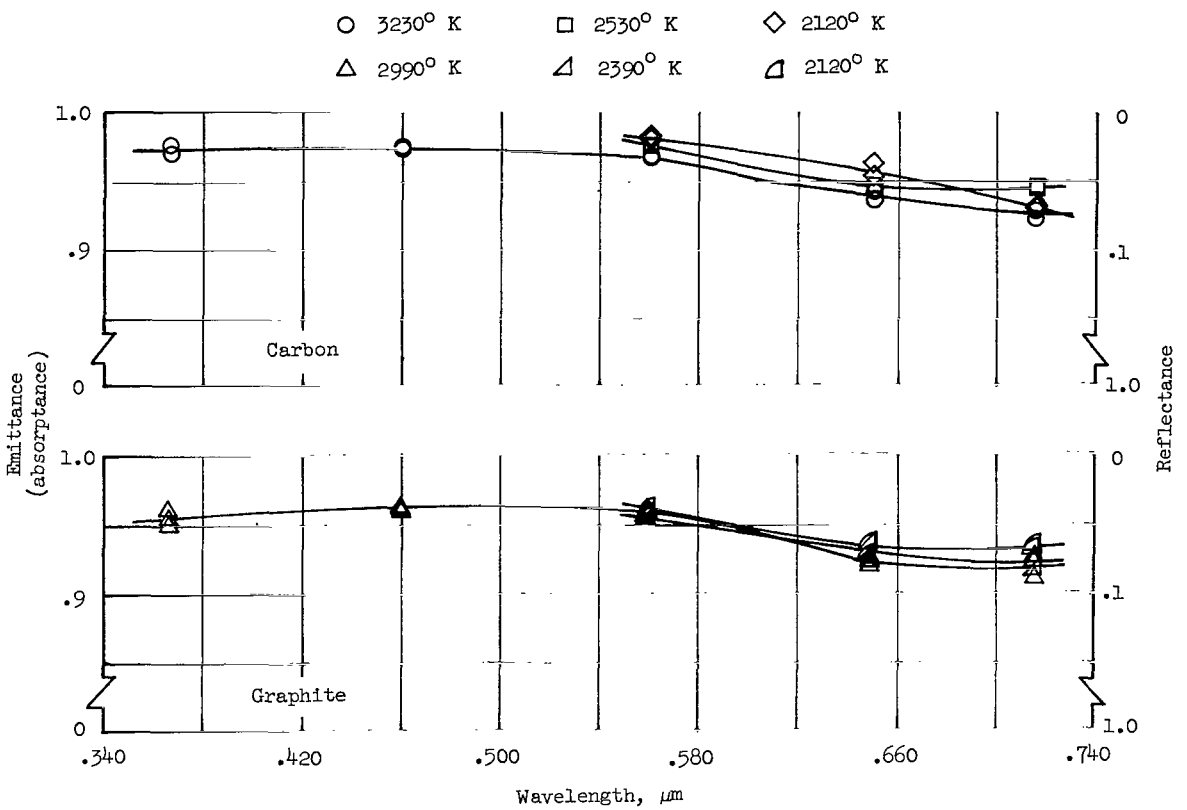

Figure 6.- Emittance and reflectance of oxidized carbon and graphite plotted against wavelength.

The values of emittance and temperature presented have been corrected for errors due to rapid cooling of the sample during chopper interruption of the arc radiation. Because of the difference between the spectral distributions of the emitted and the reflected radiation, the ratio of the emitted to reflected radiation decreases with decreasing wavelength. Consequently, the error in reflectance measurement due to rapid cooling is less at shorter wavelengths. Emittance corrections for carbon and graphite were as great as 6 percent at the highest temperature and corresponding longest wavelength and as small as 0.1 percent at the lowest temperature and shortest wavelength. It was determined by using the corrected emittance values that the average temperature drop

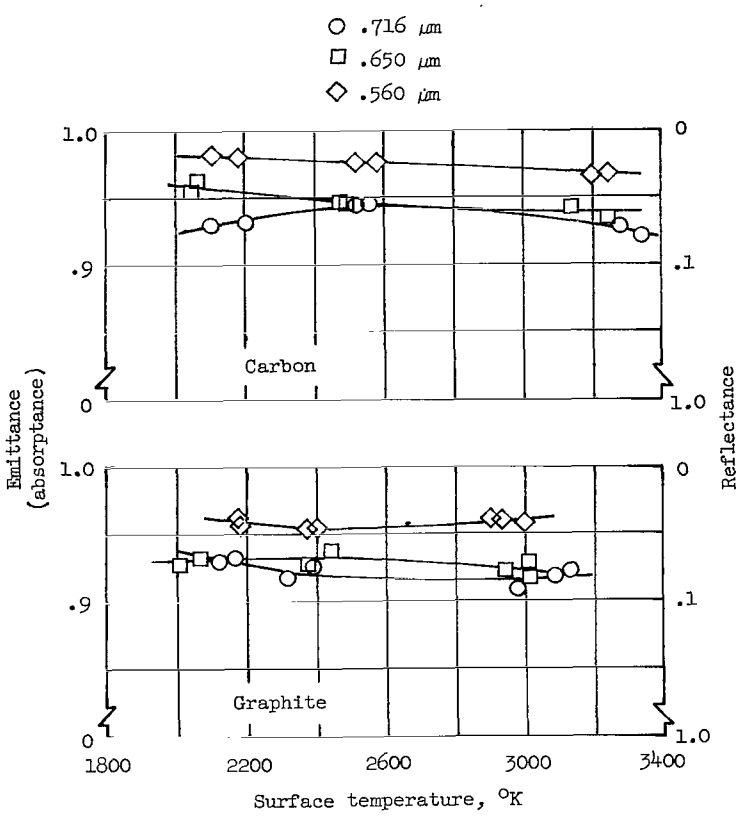

Figure 7.- Emittance and reflectance of oxidized carbon and graphite plotted against temperature.

during chopper closure was about 75° K for carbon at the highest temperature level and about 60° K at the lowest level. Graphite experienced about the same amount of cooling.

The emittance determined at the highest temperature levels is nearly constant for both graphite and carbon from 0.37 μm to 0.56 μm; it is about 0.97 for carbon and about 0.96 for graphite. Beyond 0.56 μm the emittance decreases for both materials to about 0.92. At lower temperatures the materials also show a decrease in emittance with increasing wavelength and a very slight tendency toward decreasing emittance with increasing temperature. These characteristics have been observed at lower temperatures by a number of other investigators, although considerable discrepancy in the literature exists. (See refs. 24 and 25.) A similar study on the same grades of carbon and graphite by Null and Lozier (ref. 18) produced values of emittance in close agreement with those obtained in this investigation. Null and Lozier made directional measurements of spectral reflectance at a 45° angle from the normal to the material surface for conditions of hemispherical illumination on roughened and polished samples. Although no data beyond 0.60 μm are reported in reference 18, it is indicated that a trend toward decreasing emittance for longer wavelengths was observed.

Surface-character dependence.- Spectral reflectance measurements at 0.65 μm similar to those just described were made on carbon samples, with the 20-mesh filter attenuating the irradiation, but the samples were partially protected from oxidation in order to obtain measurements on surfaces having a variety of roughnesses. By forcing a constant stream of helium tangentially across the irradiated surface of each sample and allowing different exposure times for different samples, reflectance measurements were obtained on surfaces ranging from polished to well oxidized. There was no temperature dependence for any of the reflectance data over the range of exposure times, from 5 seconds to 60 seconds, since the final reflectance measurement in every case (corresponding to the maximum temperature for the given exposure time) was always repeated in a 5-second reexposure under the protective conditions.

The emittance of each carbon sample rose rather abruptly from about 0.70 for a polished surface to about 0.90 upon initial oxidation, and then rose more slowly to 0.97 as further oxidation occurred. Upon making observations of the oxidized carbon samples with the light-section microscope, it was found that the large change in emittance from 0.70 to 0.90 occurred for a corresponding change in roughness that was not measurable with the light-section microscope, that is, a change from a polished surface to a matt surface having a roughness of the order of 1 μm. Surface-profile data were obtained, in accordance with the procedure described previously, on the more severely oxidized carbon samples, which had roughnesses greater than 1 μm. For these samples it was found that the emittance from about 0.92 to 0.97 was a linear function of the root-mean-square slopes of the surfaces, as can be seen from figure 8 in which each circle represents one test sample.

In order to determine whether the average deviation of the surface from the mean surface level was a parameter meaningful to the hemispherical spectral emittance of carbon, the arithmetic average deviation was calculated. There was no apparent correlation between this parameter and the emittance. The range of values for the arithmetic average deviation was from 4 to 17 μm.

After root-mean-square slope had been identified as an important surface-roughness parameter for carbon, values of the rms slope were determined for a typical sample of carbon and graphite representing each set of test conditions for earlier measurements in air, that is, for each temperature level represented in figures 6 and 7. These values of the rms slope are given in table 2, along with emittance data at a wavelength of 0.65 μm. The data in table 2 on carbon are not expected to fit the linear plot in figure 8, since they are slightly dependent on temperature as well as on surface roughness. Likewise the tabular data on graphite are not divorced from temperature dependence.

Measurements on Zirconia

Diamond-wheel-ground samples.- Spectral emittance and reflectance data were obtained on samples machined from calcia-stabilized zirconia (94.57 percent ZrO_2; 3.73 percent CaO). The sample surfaces were ground with a D220-N100-M $\frac{1}{8}$ diamond wheel. It has been reported by Cox (ref. 26) that the thickness of

TABLE 2.- ROOT-MEAN-SQUARE SLOPES OF SURFACES FOR REFLECTANCE MEASUREMENTS IN AIR

Material	Temperature, °K	Spectral emittance at $\lambda = 0.65$ μm	Root-mean-square slope
Carbon	3144	0.942	0.47
Carbon	2492	.946	.71
Carbon	2068	.963	.58
Graphite	3018	.918	.78
Graphite	2375	.928	1.24
Graphite	2067	.933	.92
ZrO_2 (ground)	2777	.923	.94
ZrO_2 (150F-GB)	2732	.917	1.07
ZrO_2 (120-150 GB)	2692	.905	1.06
ZrO_2 (90-120 GB)	2680	.920	.86

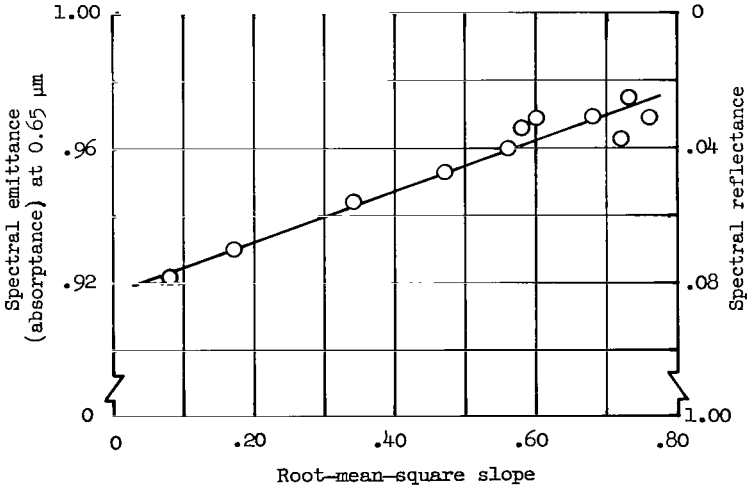

Figure 8.- Emittance and reflectance of oxidized carbon plotted against rms slope for constant temperature (<2000° K).

zirconia required for opacity to visible radiation varies from about 0.41 centimeter at room temperature to 0.13 centimeter at the melting point, which indicates that the thickness of the samples used in this investigation was sufficient to assure the validity of equation (1) for this material. Attenuation of the arc irradiation with the 10-mesh filter produced an arc image that was sufficient to melt only a small spot about 0.3 centimeter in diameter on the center of the sample surface. Under these conditions the temperature measured would be expected to be very close to the melting point. The temperature values measured at four different wavelengths ranging from 0.46 μm to 0.72 μm averaged 3009° K, with only a 1.5-percent maximum deviation from this value for the eight tests shown in the lower curve of figure 9. The value obtained for the melting point of zirconia is in reasonably close agreement with reported values for calcia-stabilized zirconia of approximately the same chemical composition. These data have been corrected for rapid-cooling errors discussed previously. Emittance corrections were as high as about 7 percent at the longest wavelength and as low as 0.4 percent for the shortest wavelength. Average temperature drop due to cooling during chopper closure was determined to be about 60° K.

Emittances and temperatures were also determined for diamond-wheel-finished samples of zirconia at a lower temperature level obtained by attenuating the arc irradiation with the 20-mesh filter. The emittance corrections for rapid cooling for these tests varied from about 5 percent to 0.3 percent and average

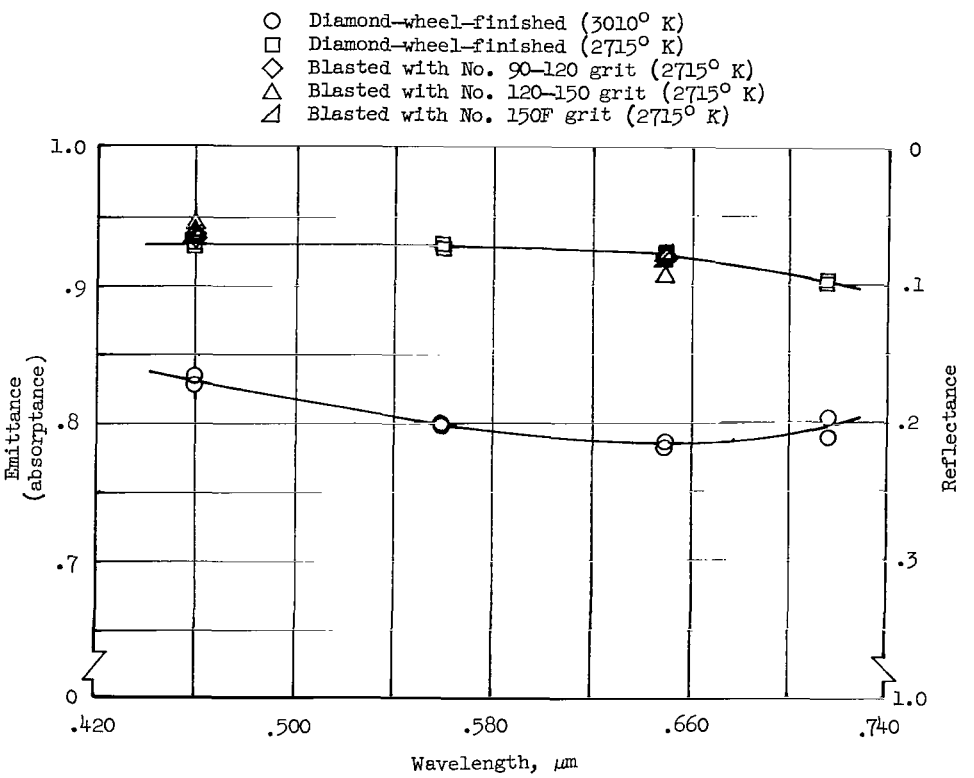

Figure 9.- Emittance and reflectance of zirconia plotted against wavelength.

cooling during chopper closure was about 55° K. The results of these tests are shown as a function of wavelength in the upper curve of figure 9. Few spectral emittance data are available on zirconia at temperatures above 2500° K. Cox (ref. 26) reports measurements at 0.665 μm at 2670° K obtained at about 45° with respect to the surface normal. These data are about 10 percent lower than those obtained in the present investigation; however, the accuracy of the measurements in reference 26 is estimated to be only ±20 percent.

Grit-blasted samples.- Special roughness treatments were given to samples of the diamond-wheel-finished zirconia in an attempt to provide samples with three additional grades of roughness. Samples were grit-blasted with number 90-120 ZrO_2 grit, number 120-150 grit, and number 150F grit. However, because of the porous nature of the zirconia, even the diamond-wheel-ground surface was comparatively rough, and the visual differences in appearance among the three grit-blasted surfaces were not very pronounced. Reflectance was measured, with the 20-mesh filter attenuating the arc irradiation in order to maintain surface temperatures below the melting point at wavelengths of 0.46 and 0.65 μm. Reflectance measurements on the three grit-blasted surfaces were essentially the same at each wavelength and did not differ significantly from the values measured on the ground surfaces, as can be seen in figure 9.

Surface profile data were obtained on zirconia samples with the four nominally different roughnesses. Root-mean-square slopes were calculated and are given in table 2. Since the rms slopes of the grit-blasted surfaces differ by no more than 14 percent from the slope of the ground surface, the roughness studies on zirconia are inconclusive, respecting the possible existence of any relationship between emittance and rms slope. However, an additional factor not present in the case of carbon is the transmission of zirconia for small thicknesses of the material. Microscope studies indicated that the sizes of irregularities in the zirconia surfaces were small compared with the thickness reportedly required for opacity. If light transmission is high for such small irregularities, it would appear that the roughness would have little influence on the emittance.

Porosity.- As a part of the physical description and identity of the zirconia studied, a pore-size spectrum was determined by the procedure described earlier and it is shown in figure 10. This figure shows the pore volume per unit volume of zirconia for given ranges of pore diameter which vary from 4 μm to 100 μm.

Measurements on Phenolic-Nylon Ablation Char

Wavelength and temperature dependence.- The ablation material studied in this program of tests was a phenolic-nylon. The phenolic-nylon was molded from a mixture of 50 percent by weight of nylon powder of 30 mesh average particle size and 50 percent by weight of powdered phenolic resin. The density in molded form was 1.21×10^3 kg/m^3. The phenolic-nylon was heated by two different methods to form char residues. In one method the material was heated in an oven constantly purged with nitrogen at a pressure slightly greater than atmospheric. The oven temperature was controlled to produce an average rate of temperature

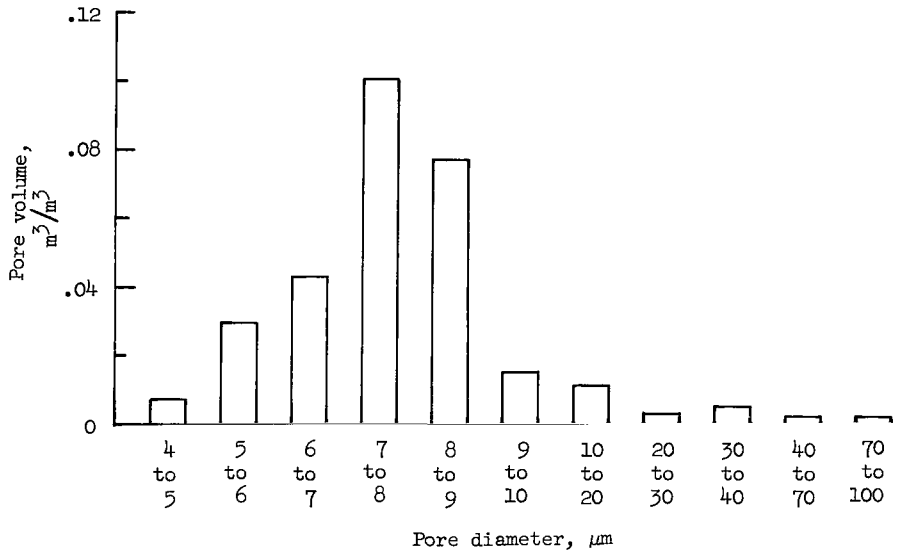

Figure 10.- Pore-size spectrum for zirconia.

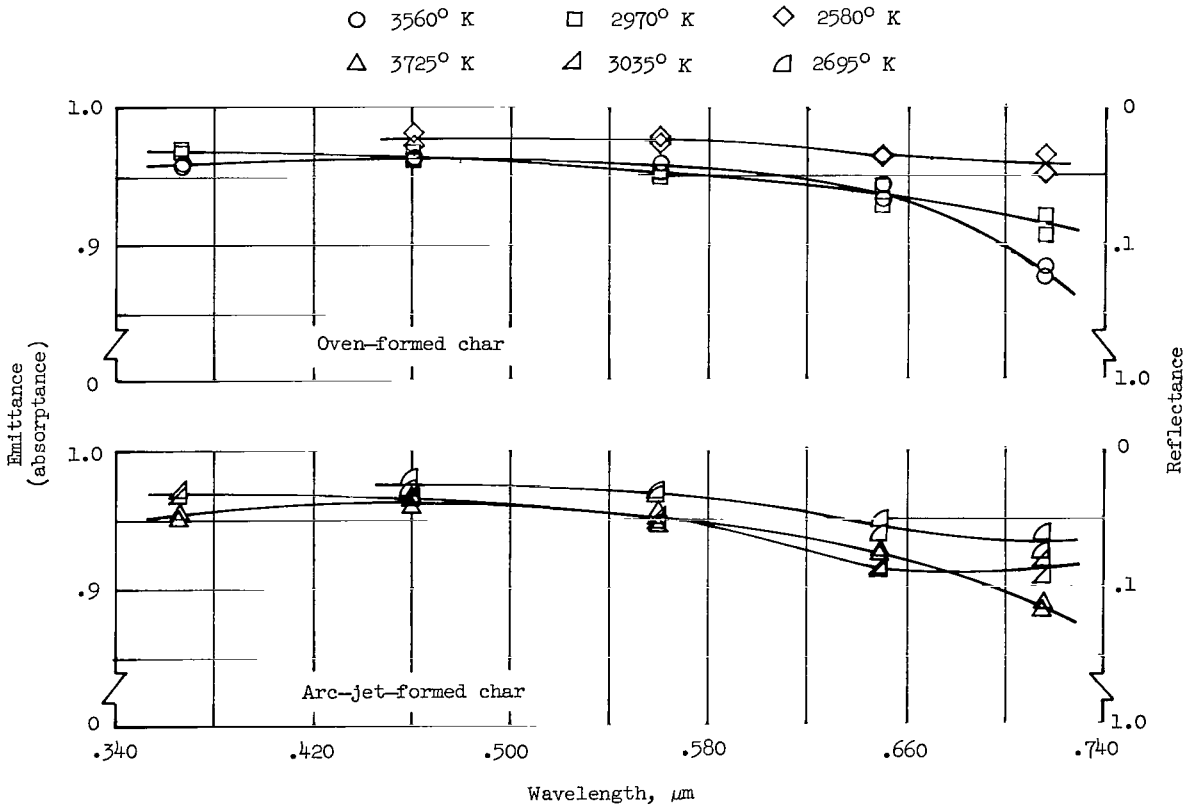

Figure 11.- Emittance and reflectance of phenolic-nylon char plotted against wavelength.

rise of about 40° K/hr until the material reached 1100° K. The material was maintained at this temperature for 3 hours and then was cooled to room temperature at a rate equal to the temperature-rise rate. The phenolic-nylon was charred in cylindrical form and the charred cylinders were subsequently cut into disks for emittance samples. These disks were given no special surface treatments, since their porosity determined their surface character. The density of the char was 0.61×10^{3} kg/m^{3}.

In the other method of forming char, 7.6-centimeter-diameter disks of the phenolic-nylon were exposed to an electric-arc-heated subsonic stream of nitrogen for 165 seconds, the time required to produce a char layer about 0.5 centimeter thick. The arc jet, described in reference 2, produced an aerodynamic thermal flux of about 1.13 MW/m^{2} on the phenolic-nylon disks. The maximum surface temperature attained by the char layers during their formation was about 2000° K. The density of the chars was 0.34×10^{3} kg/m^{3}. Disks of 1.3-centimeter diameter were cut from the char layers for emittance samples. The disks were given no special surface preparation, and reflectance measurements were made on the surface that had been exposed to the arc-heated nitrogen stream.

The emittance and reflectance of the chars at different temperatures (averaged) are shown as a function of wavelength in figure 11 and at different wavelengths as a function of surface temperature in figure 12. In general, the emittance of the oven-formed char is very slightly higher than that of the arc-jet-formed char. The slight difference between the emittance characteristics of the two forms of char may be attributable to certain physical differences observed. The oven-formed char appeared to be homogeneous, whereas the arc-jet-formed char had a cellular or columnar structure which resulted from the unidirectional flow of gases from the zone of reaction through the char layer during its formation. The densities of the char also were considerably different. The emittance characteristics of both forms of char bear a resemblance to

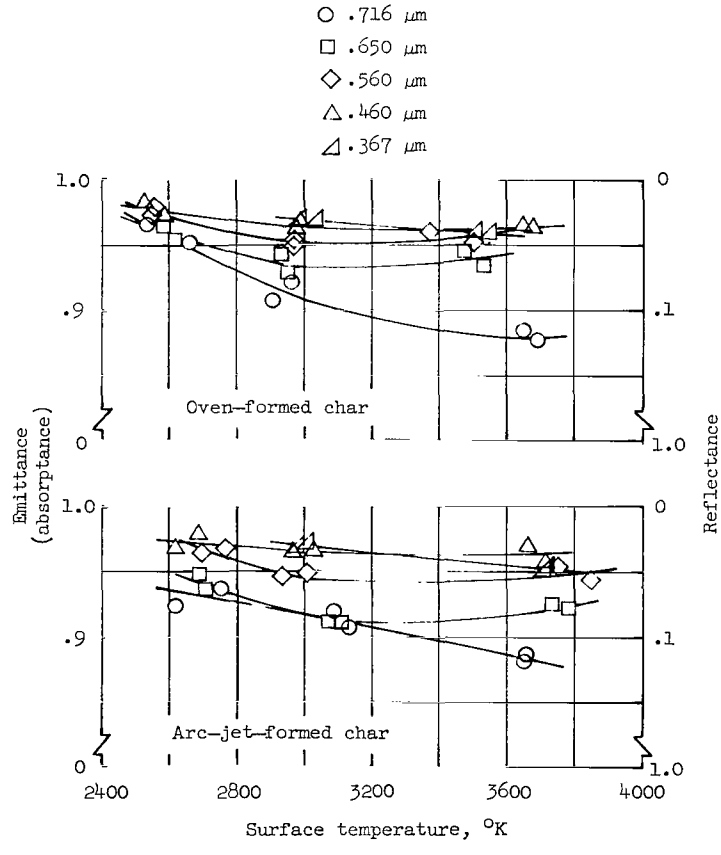

Figure 12.- Emittance and reflectance of phenolic-nylon char plotted against temperature.

those of carbon and graphite in that the emittance drops in the red region of the spectrum and also tends to drop with increasing temperature. These resemblances are not surprising, inasmuch as the chars themselves are carbonaceous.

The emittance and temperature data on the chars have been corrected for errors due to rapid cooling during chopper interruption of the arc radiation. The errors ranged from as high as 12 percent at the highest temperature and longest wavelength to no more than 0.2 percent for the lowest temperature and shortest wavelength. Cooling during chopper closure ranged from an average of 150° K at the highest temperature level to 90° K at the lowest level.

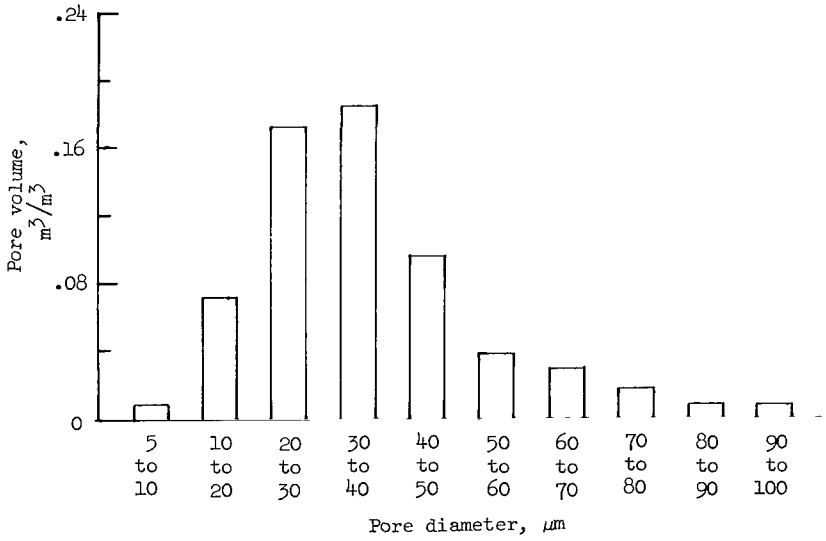

Figure 13.- Pore-size spectrum for oven-formed phenolic-nylon char.

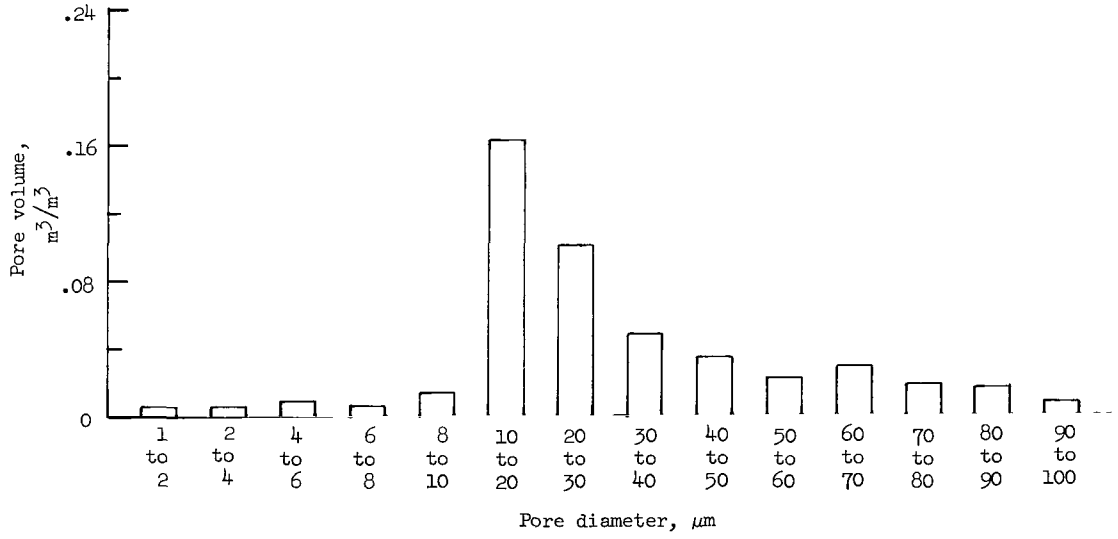

Figure 14.- Pore-size spectrum for arc-jet-formed phenolic-nylon char.

Porosity.- Because of the very porous and precipitous nature of the char surfaces it was not possible to obtain continuous profile measurements with the light-section microscope, and it seems likely that it would be difficult to obtain conventional surface parameters by other roughness-measurement techniques. Porosity measurements seemed to be more basic to the physical nature of these materials. Pore spectra on typical char emittance samples obtained after their exposure in the arc-imaging furnace are shown in figures 13 and 14.

Porosimetry studies of the chars indicated the presence of some small pores in the char samples prior to exposure in the arc-imaging furnace which were absent after exposure. It seems likely that internal oxidation of the chars during exposure in the arc-imaging furnace was responsible for changing the pore spectra, since there was a concomitant reduction in density of about 15 percent.

CONCLUDING REMARKS

Spectral hemispherical reflectance and emittance of carbon, graphite, zirconia, and a phenolic-nylon ablation char were determined with an apparatus consisting of an image pyrometer integrated with an arc-imaging furnace. Measurements on carbon and graphite included the wavelength range for which unidirectional measurements had been made recently by other investigators, but the present investigation was extended to shorter and longer wavelengths. Within the common wavelength range close agreement exists between the two sets of data. The spectral emittance determined at the 3000° K level is nearly constant for both carbon and graphite from wavelengths of 0.37 μm to 0.56 μm - about 0.97 for carbon and 0.96 for graphite. Beyond 0.56 μm the emittance decreases for both materials to about 0.92. At lower temperatures down to 2100° K, the materials also show a decrease in emittance with increasing wavelength and a very slight tendency toward decreasing emittance with increasing temperature.

Phenolic-nylon char was shown to have emittance characteristics in the visible spectrum very similar to those of carbon and graphite. The emittance characteristics of the char were shown to be relatively insensitive to the method of formation of the char, whether it be by an aerodynamic heating method or by a static (oven) heating method.

The emittance of zirconia was found to decrease slowly from the ultraviolet region to the red region of the spectrum and to be a sensitive function of temperature in the temperature region approaching and including the melting point. The temperature of melting measured for zirconia was about 3000° K, which is consistent with reported values for zirconia of similar chemical composition.

Special consideration was given to characterization of the surfaces of the materials studied. Pore-size spectra were determined for the appropriate materials. It was shown that the hemispherical spectral emittance of oxidized carbon at a wavelength of 0.65 μm is a linear function of the root-mean-square slope of the surface when the roughness is large compared with wavelength. This result appears to be significant, and it warrants further exploitation of this

surface parameter for other materials. It was also shown that changes in surface roughness of carbon which lie in the roughness region of less than approximately 1 μm change the emittance much more significantly than changes in the roughness lying in the region above 1 μm. The latter result indicates that surface irregularities of magnitude comparable with or smaller than the wavelength influence emittance most strongly, and that polished and nearly polished surfaces should be given special attention in further investigations of the relationship between surface roughness and emittance.

Langley Research Center,
National Aeronautics and Space Administration,
Langley Station, Hampton, Va., November 13, 1964.

REFERENCES

1. Brooks, William A., Jr.; Wadlin, Kenneth L.; Swann, Robert T.; and Peters, Roger W.: An Evaluation of Thermal Protection for Apollo. NASA TM X-613, 1961.

2. Peters, Roger W.; and Wilson, R. Gale: Experimental Investigation of the Effect of Convective and Radiative Heat Loads on the Performance of Subliming and Charring Ablators. NASA TN D-1355, 1962.

3. Camm, J. C.; Kivel, B.; Taylor, R. L.; and Teare, J. D.: Absolute Intensity of Non-Equilibrium Radiation in Air and Stagnation Heating at High Altitudes. J. Quant. Spectry. & Radiative Transfer, vol. 1, no. 1, Sept. 1961, pp. 53-75.

4. Mechtly, E. A.: The International System of Units - Physical Constants and Conversion Factors. NASA SP-7012, 1964.

5. Glaser, Peter E.: Imaging-Furnace Developments for High-Temperature Research. J. Electrochem. Soc., vol. 107, no. 3, Mar. 1960, pp. 226-231.

6. Comstock, Daniel F., Jr.: Method for Temperature and Reflectance Determination in an Arc-Imaging Furnace. Temperature - Its Measurement and Control in Science and Industry. Reinhold Pub. Corp., c.1962, pp. 1063-1071.

7. Abbott, E. J.; and Goldschmidt, Edgar: Surface Quality - A Review of "Technische Oberflächenkunde" by G. Schmaltz. Mech. Eng., vol. 59, no. 11, Nov. 1937, pp. 813-825.

8. Winslow, N. M.; and Shapiro, J. J.: An Instrument for the Measurement of Pore-Size Distribution by Mercury Penetration. ASTM Bull. 236, Feb. 1959.

9. Weinstein, M. A.: On the Validity of Kirchhoff's Law for a Freely Radiating Body. Am. J. Phy., vol. 28, no. 2, Feb. 1960, pp. 123-125.

10. Anon.: Standard Method of Preparation of a Magnesium Oxide Standard for Spectral Reflectivity. ASTM Designation D 986-50, Pt. 6 of 1961 Book of ASTM Standards Including Tentatives, c.1961, pp. 225-227.

11. Anon.: Preparation and Colorimetric Properties of a Magnesium-Oxide Reflectance Standard. NBS Letter Circular LC-547, U.S. Dept. Commerce, Mar. 17, 1939.

12. Middleton, W. E. Knowles; and Sanders, C. L.: The Absolute Spectral Diffuse Reflectance of Magnesium Oxide. J. Opt. Soc. Am., vol. 41, no. 6, June 1951, pp. 419-424.

13. Harrison, Thomas R.: Radiation Pyrometry and Its Underlying Principles of Radiant Heat Transfer. John Wiley & Sons, Inc., c.1960.

14. De Vos, J. C.: A New Determination of the Emissivity of Tungsten Ribbon. Physica, vol. 20, no. 10, Oct. 1954, pp. 690-714.

15. Larrabee, Robert D.: Spectral Emissivity of Tungsten. J. Opt. Soc. Am., vol. 49, no. 6, June 1959, pp. 619-625.

16. Worthing, A. G.: Temperature Radiation Emissivities and Emittances. Temperature - Its Measurement and Control in Science and Industry. Reinhold Pub. Corp., 1941, pp. 1164-1187.

17. Blau, Henry H., Jr.; Chaffe, Eleanor; Jasperse, John R.; and Martin, William S.: High Temperature Thermal Radiation Properties of Solid Materials. AFCRC-TN-60-165, U.S. Air Force, Mar. 1960.

18. Null, M. R.; and Lozier, W. W.: Research and Development on Advanced Graphite Materials. Volume XXI. Carbon Arc Image Furnace Studies on Graphite. WADD-TR-61-72, Vol. XXI, Nov. 1963.

19. Barkas, W. W. (With appendix by R. F. S. Hearmon): Analysis of Light Scattered From a Surface of Low Gloss Into its Specular and Diffuse Components. Proc. Phys. Soc., vol. 51, Mar. 1939, pp. 274-295.

20. Bennett, H. E.; and Porteus, J. O.: Relation Between Surface Roughness and Specular Reflectance at Normal Incidence. J. Opt. Soc. Am., vol. 51, no. 2, Feb. 1961, pp. 123-129.

21. Porteus, J. O.: Relation Between the Height Distribution of a Rough Surface and the Reflectance at Normal Incidence. J. Opt. Soc. Am., vol. 53, no. 12, Dec. 1963, pp. 1394-1402.

22. Davies, H.: The Reflection of Electromagnetic Waves From a Rough Surface. Proc. Inst. Elec. Eng. IV, vol. 101, Aug. 1954, pp. 209-214.

23. Anon.: Surface Texture - Surface Roughness, Waviness and Lay. ASA B46.1-1962, ASME, c.1962.

24. Plunkett, J. D.; and Kingery, W. D.: The Spectral and Integrated Emissivity of Carbon and Graphite. Proceedings of the Fourth Conference on Carbon, Pergammon Press, New York, 1960, pp. 457-472.

25. Thorn, R. J.; and Winslow, G. H.: Radiation of Thermal Energy From Real Bodies. Temperature - Its Measurement and Control in Science and Industry, vol. 3, pt. 1, F. G. Brickwedde, ed., Reinhold Pub. Corp., c.1962, pp. 421-448.

26. Cox R. L.: A Technique for Measuring Thermal Radiation Properties of Translucent Materials at High Temperature. Measurement of Thermal Radiation Properties of Solids. Joseph C. Richmond, ed., NASA SP-31, 1963, pp. 469-481.

"The aeronautical and space activities of the United States shall be conducted so as to contribute . . . to the expansion of human knowledge of phenomena in the atmosphere and space. The Administration shall provide for the widest practicable and appropriate dissemination of information concerning its activities and the results thereof."

—NATIONAL AERONAUTICS AND SPACE ACT OF 1958

NASA SCIENTIFIC AND TECHNICAL PUBLICATIONS

TECHNICAL REPORTS: Scientific and technical information considered important, complete, and a lasting contribution to existing knowledge.

TECHNICAL NOTES: Information less broad in scope but nevertheless of importance as a contribution to existing knowledge.

TECHNICAL MEMORANDUMS: Information receiving limited distribution because of preliminary data, security classification, or other reasons.

CONTRACTOR REPORTS: Technical information generated in connection with a NASA contract or grant and released under NASA auspices.

TECHNICAL TRANSLATIONS: Information published in a foreign language considered to merit NASA distribution in English.

TECHNICAL REPRINTS: Information derived from NASA activities and initially published in the form of journal articles.

SPECIAL PUBLICATIONS: Information derived from or of value to NASA activities but not necessarily reporting the results of individual NASA-programmed scientific efforts. Publications include conference proceedings, monographs, data compilations, handbooks, sourcebooks, and special bibliographies.

Details on the availability of these publications may be obtained from:

SCIENTIFIC AND TECHNICAL INFORMATION DIVISION

NATIONAL AERONAUTICS AND SPACE ADMINISTRATION

Washington, D.C. 20546